

# Structural and Magnetic properties of Strontium Hexa-Ferrites for Permanent Magnets

K. Alamelu Mangai, Dr. P. Sureshkumar., Dr. M. Priya., Dr. M. Rathnakumari

## **Abstract**

Nanoparticles of strontium ferrites with nominal composition  $\text{SrFe}_{12}\text{O}_{19}$  were prepared by sol-gel method. The as-synthesized sample was characterized by thermo gravimetric analysis, X-ray diffraction (XRD), scanning electron microscopy (SEM), energy dispersive spectroscopy (EDS) and Tunneling electron microscopy (TEM). The X-ray powder diffraction results showed that the sample was single phase with the space group of P63/mmc. The lattice constants' almost remains constant. The crystallite size obtained from XRD data is in the range of 10nm the sample annealed at 800°C. Most of the particles formed had hexagonal structure, as observed by the scanning electron microscopy and The average grain size as determined was found in the range of 35nm. The hexagonal needle-like morphology was obtained by TEM photograph. The crystallite size estimated from X-rays diffraction data was in the range 10nm, which is much smaller than that already reported. The M-H loop indicated that both coercivity and saturation magnetization were 6405 Gauss and 28.26emu/g observed at 800°C. This coincides with theoretical limit. The yield percentage along with structure determination and VSM studies of the prepared samples will be discussed in detail.

**Index Terms**—Hardferrite; Nanoparticle; Magnetic properties; TEM; VSM;

## **1. Introduction:**

Ferrites are ferrimagnetic ceramic materials that can be magnetized to produce large magnetic flux densities in response to small applied magnetic forces. Magnetic materials mainly fall in to two groups with different crystal structures: cubic, Hexagonal. The most important in hexagonal group are barium and strontium ferrites,  $\text{Ba}_0.6\text{Fe}_2\text{O}_3$  and  $\text{Sr}_0.6\text{Fe}_2\text{O}_3$ , which are magnetically hard. They are considered better than other magnetic materials because they have high electrical resistivity and low eddy current losses [1].

Magnetic nanomaterials are used in sound and data storage technology, micro motors for cassette and video tape recorders, television technology, generators, speaker magnets, magnet clamps and retainers for mechanical engineering, and magnetic snap-lockstrips for furniture and refrigerators [2]. Also, used in information recording and storage systems, in new permanent magnets [4], in magnetic cooling systems, as magnetic sensors, etc. The most successful application of nanomagnetism has been to magnetic recording [5], which has taken this technology through a swift evolution in the last 5 decades.

The magnetic behavior of nanoparticles is, in general, strongly dependent on their dimensions. For example, the smaller magnetically ordered particles will tend to be single-domain, and the larger ones, above a certain critical diameter  $D_{cr}$ , will be multidomain, or else exhibit a vortex configuration, an arrangement where

the local magnetizations are aligned tangentially to circles. Magnetic nanoparticles also have other properties that depend on their sizes.

The sol-gel synthesis technique employing ethylene glycol as the gel precursor has been widely attempted on the M-type ferrites. The synthetic technique has been successful in producing homogeneous nanosized ferrite crystallites at a much lower calcination temperature. It is known that calcination temperature will affect the crystalline size and ultimately the properties of the produced ferrites [6]. Traditionally, solgel process involves hydrolysis and condensation of metal alkoxides and an alkoxide ion is the conjugate base of an alcohol. The general synthesis of metal alkoxides involves the reaction of metal species (a metal, metal hydroxide, metal oxide, or metal halide) with an alcohol. Metal alkoxides are good precursors because they readily undergo hydrolysis; that is, the hydrolysis step replaces an alkoxide with a hydroxide group from water and a free alcohol is formed. Factors that need to be considered in a sol-gel process are solvent, temperature, precursors, catalysts, pH, additives, and mechanical agitation. These factors can influence the kinetics, growth reactions, hydrolysis, and condensation reactions [7]. At 600 °C, mixed products consisting of hematite,  $\alpha\text{-Fe}_2\text{O}_3$  and M-type  $\text{SrFe}_{12}\text{O}_{19}$  were obtained. As the calcination temperature increased above 600 °C, there was an decrease in particle size but this increased when the temperature is increased beyond 800 °C [8].

## **2. Experimental Procedure:**

The synthesis of  $\text{SrFe}_{12}\text{O}_{19}$  was performed using sol-gel route. Ethylene glycol ( $\text{C}_2\text{H}_6\text{O}_2$ ) was used as the solvent and gel precursor where stoichiometric weight of  $\text{Sr}(\text{NO}_3)_2$  and  $\text{Fe}(\text{NO}_3)_3 \cdot 9\text{H}_2\text{O}$  (as the stoichiometric ratio of Fe/Sr is 1:4) was dissolved at a temperature of  $50^\circ\text{C}$  for 2 h with continuous stirring using a magnetic stirring bar. The homogeneous solution was then placed on top of a hotplate with the magnetic stirring bar removed for dehydration to occur as this enhanced the gelation process. Slow dehydration occurred over 72–96 h at the temperature range of  $100^\circ\text{C}$  and subsequently a dried gel was obtained. The dried gel, which contained finely mixed oxides of the starting materials, was then calcined at the desired temperatures for 96 h at atmospheric condition in a muffle furnace with an intermediate grinding after each 48-hour cycle of calcination, and was then quenched in air.

XRD patterns were collected using  $\text{Cu-K}\alpha$  radiation from XRD Lab-NIIST, Trivandrum and were matched using an automated XRD software package, which includes the standard JCPDS files. The Scanning electron microscopy (SEM) and FESEM micrographs was carried out for the sample calcined at  $800^\circ\text{C}$  to determine the grain size and morphology of the product. The magnetic properties of the product is observed using Vibrating Sample Magnetometer at room temperature.

### 3. Results and discussion:

#### 3.1. TG/DTA Study:

Fig.1 shows TG/DTA analysis spectrum of the as synthesized sample. There is a mass loss effects in thermogravimetric curve (TG curve). The excellent hydroscopic property of the dried gel, which is relative to the big specific surface area and the porous and loose structure of the precursor nanoparticles, is confirmed by the great deal of mass loss in the temperature range of  $30^\circ\text{C}$  to  $400^\circ\text{C}$ . The mild mass loss in the temperature range of  $400^\circ\text{C}$  to  $750^\circ\text{C}$  is due to the decomposition products and no weight gain is observed in the temperature of above  $800^\circ\text{C}$  under nitrogen atmospheric condition which is best suited in the recent investigation [11].

The differential thermal analysis curve in Fig.2. Shows the endothermic and exothermic effects of as-synthesized sample in nitrogen atmosphere in the temperature range of 25– $1000^\circ\text{C}$  at a ratio of  $20^\circ\text{C}/\text{min}$ . The intense endothermic effect at  $70^\circ\text{C}$  shows

that the free water in the dried gel may mainly occur on the gel particles and in the macro and meso pores. The weak endothermic effect at  $288^\circ\text{C}$  illustrates that a little free water may be in the micro pores and capillaries. The endothermic effect at about  $717^\circ\text{C}$  between two exothermic effects occurring at  $650^\circ\text{C}$  and  $769^\circ\text{C}$  may result from the endothermic decomposition of the strontium M-type hexaferrite nanoparticles. The exothermic effects in the temperature ranges of  $197^\circ\text{C}$  and  $361^\circ\text{C}$  was observed.

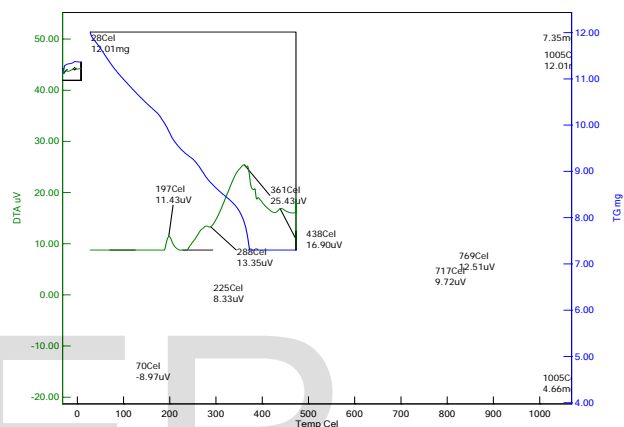


Fig.1. TG/DTA plots of as-synthesized  $\text{SrFe}_{12}\text{O}_{19}$  sample

#### 3.2. XRD Investigation:

Fig. 2 showed the XRD patterns for the sample which was calcined at  $800^\circ\text{C}$ . All the reflections were indexed on the basis of the M-type structure retaining the  $\text{P63}/\text{mmc}$  space group, with the initial cell parameters of  $a=5.886 \text{ \AA}$ ,  $c=23.037 \text{ \AA}$ , and the JCPDS Files had been referred to for all the peak position identification. The impurity iron oxide phase is preferentially formed when strontium content is low and at low calcination temperature. In the synthesis of M-type strontium ferrite where the ratio of Sr/Fe range is 1:4, it is anticipated that the single phase M-type Strontium Ferrite was obtained at  $800^\circ\text{C}$  and the particle size was found to be 10nm.

According to Verstegen and Stevels [9], an examination of  $c/a$  parameter ratio may be used to quantify the structure type, as the M-type structure can be assumed if the ratio is observed to be lower than 3.98. The  $c/a$  ratios were calculated for the parent ferrite; and as prepared sample which ranged from 3.927 to 3.981, are well within the ratio range of M-type structures.

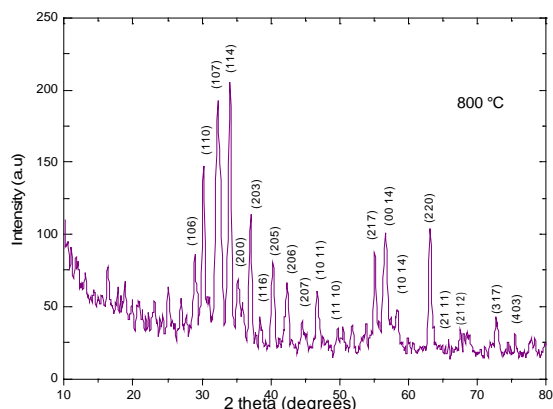


Fig.2. XRD Patterns of a series of calcinations at 800 °C of SrFe<sub>12</sub>O<sub>19</sub>

The refined lattice cell parameters calculated from the XRD patterns. Sample at 800°C showed a slight contraction in the *c*-axis and expanded in the *a*-axis resulting in an increase in 0.44% in the lattice cell volume. The average particle size of the samples was deduced from the width at half height of XRD maxima by applying the Scherrer's equation.

### 3.2.SEM images:

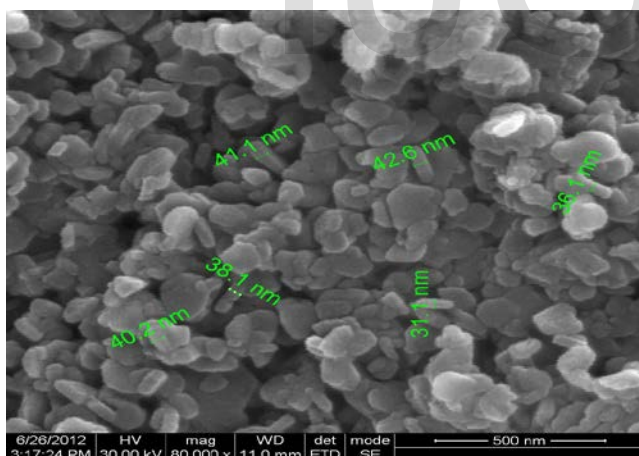


Fig.3. (a)

To illustrate the particle morphology during calcining treatment, the calcinations of the dried gel after having been heat treated at 100°C for 96 h and then calcined for again 96 h at 800°C was observed with FESEM as shown in in Fig.3. At 800°C, the nanoparticle with sizes less than 100nm, composed of single phases, showed a cluster of strontiumferrite exhibiting faceted nature of the hexagonal ferrites.

The micrograph showed clustering happened around a core center of approximately 500 nm in diameter, which represented a void space created by ethylene glycol sol. The size of the clustered particles ranged from 200 to 400 nm in dimension, and a few distinctively displayed the hexagonal faceted nature of the M-type ferrites. The micrograph proved that ethylene glycol was useful in modulating the distance between the ferrites. However, it was still unable to effectively prevent the hexaferrites from clustering together.

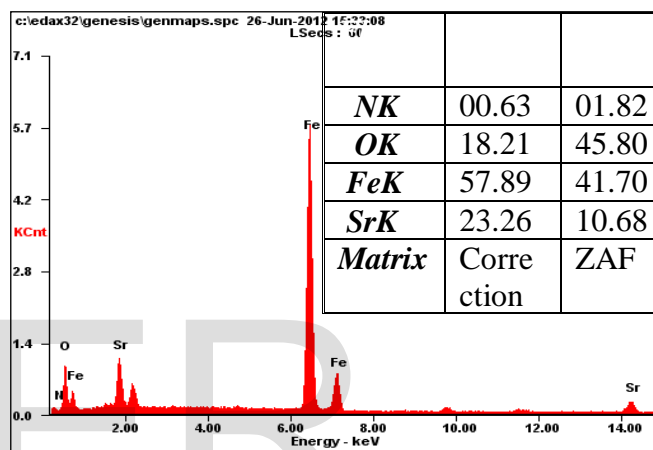


Fig.3.(b)

Fig.3 (a). FESEM micrograph & (b). EDAX Spectra for the sample calcined at 800 °C

Fig.3 reveals that the sample calcined at 800 °C have coarser grains and the particles are hexagonal platelets and well crystalline strontium ferrites. The average external diameters are in the range of around 35nm. The mean particle size of the samples are as the function of calcination temperature and the stoichiometric ratios on which the precursors were applied.

### 3.2.TEM images:

Transmission electron microscopy was employed to confirm the nanocrystalline nature of the sample. Fig.4 illustrates the TEM micrograph for the sample calcined at 800°C. It is clear observing from this image that the nanoparticles are almost hexagonal in structure. The average particle size observed from this image is 20nm, which is in accordance with the results obtained from the Scherrer formula of XRD.

From both the observations of XRD and TEM, it is clear that the particle sizes observed from TEM micrographs are large than that calculated from XRD analysis and the sample with more series aggregation leads generally to large difference between XRD and TEM measurements.

### 3.4. Magnetic Characteristics:

Magnetization measurements were carried out using VSM with an applied field of 19KOe. The VSM is very versatile and sensitive. It may be used for both weakly and strongly magnetic substances, and standard versions can detect a magnetic moment of about  $10^{25}$  emu. This corresponds to the saturation magnetization of about 0.04mg of iron, which suggests the attention to cleanliness that is necessary when measuring small or weakly magnetic samples. Magnetization Vs the applied field plots for  $\text{SrFe}_{12}\text{O}_{19}$  is shown in Fig.4. The sample calcined at 800 °C shows smooth hysteresis loop which confirms the formation of pure strontium hexaferrite.

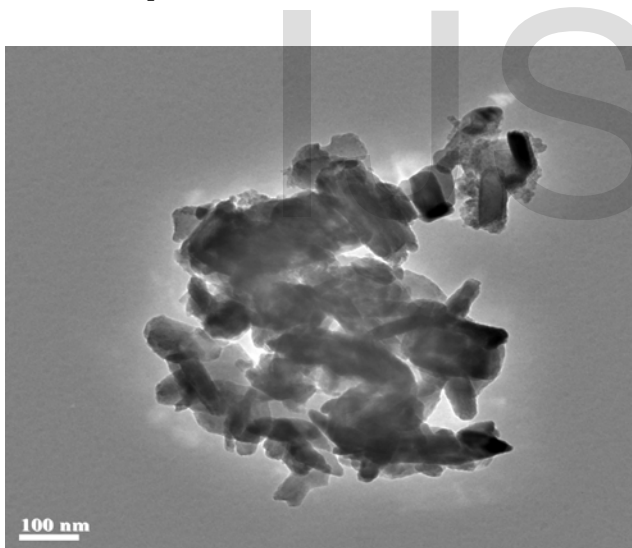


Fig.4. TEM micrograph for the sample calcined at 800 °C

The annealing temperature at 800 °C produced a hard ferrite, which has a coercivity of 6405 Oe and its saturation magnetization was 28.26 emu/g at the Field of 19KOe. The saturated Magnetization  $M_s$  and the Remenant Magnetization  $M_r$  at 800 °C were very closer to the theoretical value. Compared with other values reported in other literatures, the coercivity, saturation magnetization and Remenant magnetization was well improved by the ratio of

$\text{Sr}/\text{Fe}$  was 1:4 at 800 °C. It is known that the energy of a magnetic particle in an external field is proportional to its size via the number of magnetic molecules in a single magnetic domain. When this energy becomes comparable to thermal energy, thermal fluctuations will significantly reduce the total magnetic moment in a given field [11].

It is also known that spin-coating phenomenon can be induced near the surface by the thermal gradient between surface and bulk [12]. This phenomenon is more significant for the nanoparticles due to the large surface to volume ratio. Therefore it is reasonable that the magnetization of nanoparticles is usually smaller than that of the corresponding bulk materials.

The remenant Magnetization ( $M_r$ ) for the products calcined at 800 °C was about 15 emu/g, which remained 50% of saturation magnetization. However, it was surprised that the coercivity ( $H_c$ ) values for the product calcined at 800 °C was 6405 Gauss. This was coincides with the theoretical limit (7500 Gauss). It is known that the magnetic properties are dependent on the morphology of the particles. From Fig(5), it could be seen that the slight variation in shape anisotropy might be another reason causing the very small reduction in  $M_s$ . Thus the coercivity and magnetization was found to be improved by this ratio.

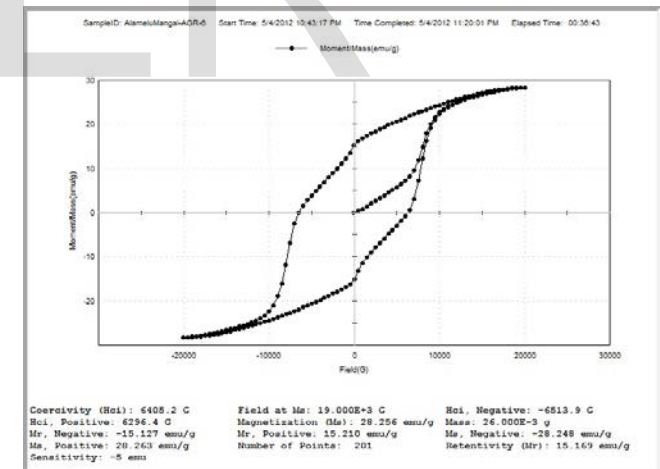


Fig.5. Hysteresis Curve for the Samples at the annealing temperature 800 °C using Vibrating Sample Magnetometer

The squareness ratio is essentially a measure of how square the hysteresis loop and is given by the ratio of ( $M_r/M_s$ ). The relative high value of SQR (40.25) suggested that the the sample may be multi-domains in nature. In general, large SQR values are desired for recording medium. The main indication of the existence of exchange bias is the shift of hysteresis

loop when in field cooling. It was reported that coercivity was increased in the miniaturization of the magnetic nanostructures; The exchange bias phenomenon observed here would most likely be defect-induced exchange bias by the existence of oxygen vacancies in the M-type structure.

#### 4. Conclusions

The calcination temperature at 800 °C produced strontium ferrite with 10nm in grain size based on the Scherrer's equation, SEM images confirmed the formation of M-type ferrite and compared the particle size with FESEM. At this temperature range the sample produces harder ferrite. Calcination temperature and the molar ratio of Sr/Fe of 1:4 plays an important role in the formation of strontium hexaferrite phase in sol-gel template method. The VSM results indicated that as the Fe<sup>3+</sup>/Sr<sup>2+</sup> stichiometric ratio and the calcination temperature were 4, 800 °C, respectively, the magnetism reached the maximum. The coercivity, saturation magnetization and remanent magnetization for the sample under the optimum conditions at 19Koe were 6405 Oe, 28.26 and 15.2 respectively.

#### References

- [1] H. Kojima, in: E.P. Wohlfarth (Ed.), *Ferromagnetic Materials*, Vol. 3, Amsterdam, 1982
- [2] O. Kubo, T. Ido, H. Yokoyama, *IEEE Trans. Magn.* 18 (1982) 1122-1124.
- [3] J. Smit, H.P.J. Wijn, *Ferrites: Physical Properties of Ferrimagnetic Oxides in Relation to their Technical Application*,
- [4] X.X. Liu, J.M. Bai, F.L. Wei, Z. Yang, A. Morisako, M. Matsunori, *J. Magn. Magn. Mater.* 212 (2000) 273-275.
- [5] Z.F. Zi, Y.P. Sun, X.B. Zhu, Z.R. Yang, J.M. Dai, W.H. Song, *J. Magn. Magn. Mater.* 320 (2008) 2746.
- [6] M.M. Hessian, M.M. Rashad, K. El-Barawy, *J. Magn. Magn. Mater.* 320 (2008) 336-344  
Philips Technical Library, 1959.
- [7] Brinker, C. J., and Sherrer, G. W., *Sol-Gel Science*, Academic Press, NY (1990)
- [8] Geok Bee Teh, Yat Choy Wong, *Journal of Magnetism and Magnetic Materials* 323 (2011) 2318-2322
- [9] T.R. Wagner, *J. Solid State Chem.* 136 (1998) 120.
- [10] G.B. Teh, Y.C. Wong, J. Wang, S.G. Tan, B. Samini, *Mater. Sci. Forum* 654-656 (2010) 1134.
- [11] K.V. P. Shafi, A. Gedanken, R. Prozorov, J. Balogh, *Chem. Mater.* 10(1998) 3445
- [12] S. Kurisu, T. Ido, H. Yokoyama, *IEEE Trans. Magn.* 23 (1987) 3137.

- K. Alamelu Mangai, *Department of Physics, Vel Tech High Tech Engineering College, India, PH-9443836550.*

E-mail: [gmangai4782@gmail.com](mailto:gmangai4782@gmail.com).

- P. Suresh Kumar Velammal Engineering College, Department of Physics, India, PH-914426811499. E-mail: [sureshrath@yahoo.com](mailto:sureshrath@yahoo.com)
- M. Priya, Dept. of Physics, Saveetha Engineering College, India, PH-9487423240, [priyam7373@gmail.com](mailto:priyam7373@gmail.com)
- M. Rathnakumari, Velammal Engineering College, Department of Physics, India, PH-9962991229. E-mail: [mrathnakumari@yahoo.com](mailto:mrathnakumari@yahoo.com)